

PARATOLUENE SULPHONIC ACID CATALYZED SOLVENT FREE GREEN SYNTHESIS OF AZO DYES WITH BIOFILM INHIBITION AND HEMOLYTIC ACTIVITY

Shazia Kousar^{*1}, Rabia Saleem², Muhammad Ahmad Mudassir^{*3}, Syed Adnan Ali Shah^{*4},
Ayesha Monwar⁵, Muhammad Shahid⁶, Madiha Irfan⁷, Saddam Hussain⁸

^{*1,2,5,7,8}Institute of Chemistry, Khwaja Fareed University of Engineering and Information Technology (KFUEIT), Rahim Yar Khan 64200, Pakistan

^{*3}Chemistry Department, University of Management and Technology (UMT), Sialkot Campus, Sialkot 51310, Pakistan

^{*4}Faculty of Pharmacy, Universiti Teknologi MARA Cawangan Selangor Kampus Puncak Alam, 42300 Bandar Puncak Alam, Selangor Darul Ehsan, Malaysia

⁶Department of Chemistry and Biochemistry, University of Agriculture, Faisalabad, Pakistan

^{*1}shazia.kousar@kfueit.edu.pk, ^{*3}ma.mudassir@kfueit.edu.pk, ^{*4}syedadnan@uitm.edu.my

DOI: <https://doi.org/10.5281/zenodo.15532217>

Keywords

Article History

Received on 15 March 2025

Accepted on 15 April 2025

Published on 30 April 2025

Copyright @Author

Corresponding Author: *

Shazia Kousar,
Muhammad Ahmad
Mudassir,
Syed Adnan Ali Shah

Abstract

A series of aryl azo dyes was synthesized through a solvent-free mechanochemical grinding approach, offering an environmentally friendly alternative to conventional synthetic methods. The process involved diazotization of aniline derivatives, followed by coupling with phenolic compounds under grinding conditions, yielding dyes with high purity and intense coloration. The reaction progress was monitored using thin-layer chromatography (TLC), and structural confirmation of the final products was carried out using FTIR and NMR Spectroscopy. The dyes displayed notable thermal stability and potential applications in textiles, sensors, and biomedicine. In addition to structural analysis, biological activity was evaluated using biofilm inhibition and hemolysis assays. Eight compounds (RS-01 to RS-08) were tested against *Bacillus subtilis* (*B. subtilis*) and *Escherichia coli* (*E. coli*). RS-08 exhibited the highest biofilm inhibition in *B. subtilis* at 76.11%, whereas RS-05 showed a slight promotion of biofilm at -1.13%. In *E. coli*, RS-05 and RS-06 demonstrated moderate inhibition (54.35% and 49.74 %, respectively), whereas RS-07 and RS-08 promoted biofilm formation, as indicated by the negative inhibition values. The hemolytic activity was assessed using human blood cells. RS-05 caused the highest hemolysis (56.2%), whereas RS-08 exhibited the lowest hemolysis (18.51%), indicating lower cytotoxicity. These findings support the potential of the selected azo dyes for biocompatible applications, with RS-08 emerging as a promising candidate owing to its potent biofilm inhibition and minimal hemolytic impact.

1. Introduction

Aryl azo dyes are a highly significant class of synthetic colorants known for their energetic chromatic properties, strong thermal and photo stability, and

extensive utility across numerous industrial fields. These compounds are structurally characterized by one or more azo linkages (-N=N-) that bridge

aromatic systems, conveying intense coloration and tunable optical behavior. Due to their notable color fastness, high molar extinction coefficients, and resistance to degradation, azo dyes are extensively employed in ink formulations, textiles, cosmetics, food additives, pharmaceuticals, and functional materials such as optoelectronic and photoactive devices [1–7].

In addition to their commercial significance, traditional synthetic routes to azo dyes are often associated with environmentally harmful practices. Diazotization-coupling reactions characteristically require hazardous aromatic amines, strong acids, and volatile organic solvents, leading to substantial chemical waste and posing risks to human health and ecosystems [8–11]. This environmental problem is increasingly viewed as unsustainable in light of modern green chemistry principles highlighting waste reduction, safer reagents, energy efficiency, and benign solvents or solvent-free conditions [12–16].

In response to these concerns, solvent-free synthesis techniques have emerged as viable alternatives to address many of the limitations of conventional protocols. In particular, mechanochemical synthesis has gained prominence for facilitating chemical transformations via mechanical energy input, typically through grinding or milling, without needing solvents [17–20]. This method has been shown to accelerate reaction rates, improve product yields, and reduce the formation of undesired by-products, while minimizing environmental hazards [21–23].

Additional solvent-free approaches, such as microwave irradiation and solid-state synthesis, have also been demonstrated. These methodologies can enhance reaction kinetics, reduce energy consumption, and encourage cleaner synthesis by avoiding traditional thermal heating and solvent-intensive conditions [24–26]. The utility of these green techniques has further expanded through the development of azo-based materials with advanced functional properties.

Recent advancements in this area have produced azo dyes with responsive electronic and photochemical behavior, making them suitable for molecular switches, nonlinear optics, and controlled drug release systems [27–29]. Their potential in designing innovative materials for applications in pH sensing,

data storage, memory devices, and adaptive coatings also demonstrates the adaptability of azo dye chemistry [30–32].

Certain azo dye derivatives have shown valuable biological activity despite their physicochemical properties. Antimicrobial, anticancer, and antifungal effects have been reported, suggesting that these compounds may have dual roles in materials and biomedical sciences [33–35]. This study explored the synthesis and biological evaluation of eight azo dyes using solvent-free mechanochemical methods. Their activities against the biofilm-forming *B. subtilis* and *E. coli* bacteria were also considered. Among the tested compounds, RS-08 exhibited significant inhibitory effects against *B. subtilis*, whereas RS-05 and RS-06 showed reasonable activity against *E. coli*. Hemolytic assays using human red blood cells were performed to evaluate cytotoxicity, with RS-08 displaying the least hemolytic effect, indicating its potential biocompatibility, whereas RS-05 showed higher cytotoxicity, warranting further toxicological analysis. This study demonstrates how green synthetic strategies with biological testing can produce multifunctional azo dyes with minimal environmental effects and potential biomedical significance. Such methodologies are dynamic in advancing sustainable chemistry while expanding the utility of azo compounds in scientific and industrial frameworks.

2. Experimental

2.1 Instruments and Chemicals

All chemicals used in this study were of analytical grade and were used without further purification. Fluorescein was obtained from Merck (Germany), and various other phenols (8-hydroxyquinoline, phenolphthalein, and 2,7-dihydroxynaphthalene), anilines, p-toluene sulfonic acid, and sodium nitrite were obtained from Sigma-Aldrich. Solvents, including methanol, dichloromethane (DCM), and ethanol, were purchased from Sigma-Aldrich. To monitor the progress of the reaction and confirm product formation, thin-layer chromatography (TLC) was performed at 30 min intervals. Silica-coated TLC plates were used, and spots were visualized under a UV lamp at 254 and 366 nm. The mobile phase for TLC consisted of DCM and methanol in a 9:1

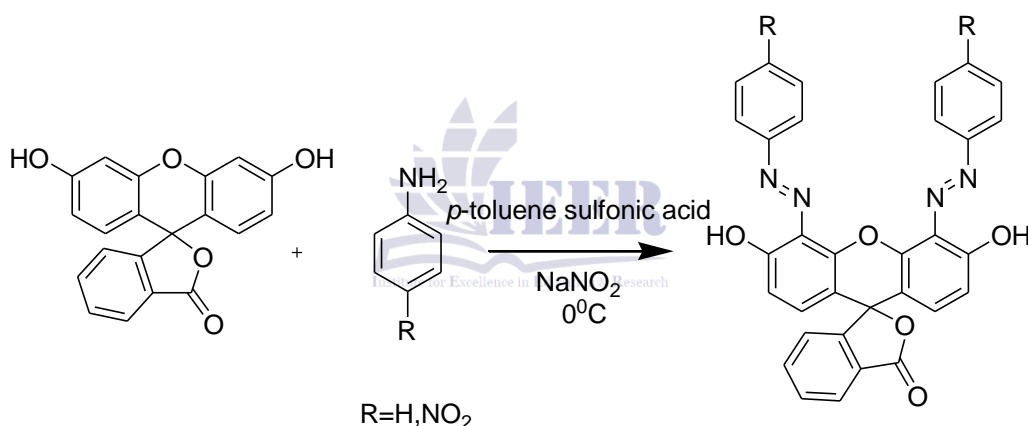
ratio. Furthermore, the NMR spectra were recorded using a 600 MHz spectrometer.

2.2 General procedure for the synthesis of aryl azo dyes

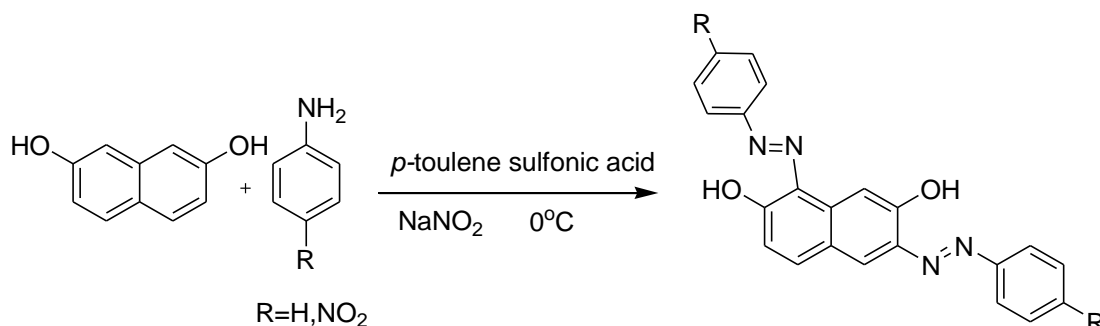
The solvent-free synthesis of aryl azo dyes was carried out under mechanochemical grinding conditions. Initially, aniline (2.12 mmol) was mixed with sodium nitrite (2.12 mmol) in the presence of *p*-toluenesulfonic acid (2.12 mmol) in an agate mortar, and grinding was performed using a pestle. The reaction mixture was maintained at 0 °C in an ice bath, allowing the diazotization reaction to proceed for 5 min.

Following diazotization, phenol (1.06 mmol) was added directly to the reaction mixture, and grinding was continued for an additional 10 min. A visible color change, ranging from yellow to red, was observed

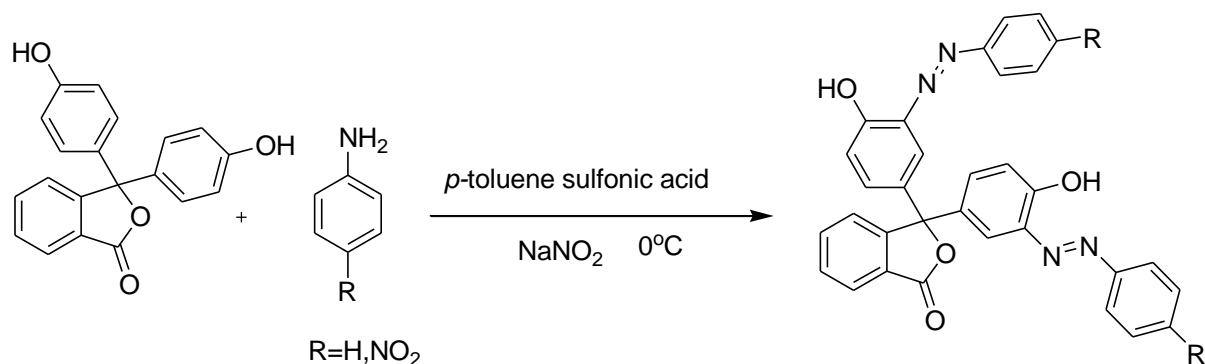
depending on the phenol used, indicating the successful coupling of the diazonium salt with the phenolic substrate. The reaction progress was monitored by TLC on silica gel plates with a mobile phase consisting of ethyl acetate/*n*-hexane (1:1 v/v). The reaction pathways for the solvent-free synthesis of aryl azo dyes are shown in **Schemes 1, 2, 3, and 4**. The resulting crude product was collected, washed with ethanol, and recrystallized to obtain a high-purity aryl azo dye. The yields of the reactions ranged from 88 to 95%, demonstrating the efficiency of this solvent-free methodology. The melting points of the purified compounds were determined using a Stuart SMP30 melting point apparatus, revealing the decomposition temperature characteristics of the azo compounds. "Table 1 presents the melting points of the synthesized aryl azo dyes, demonstrating their thermal stability."



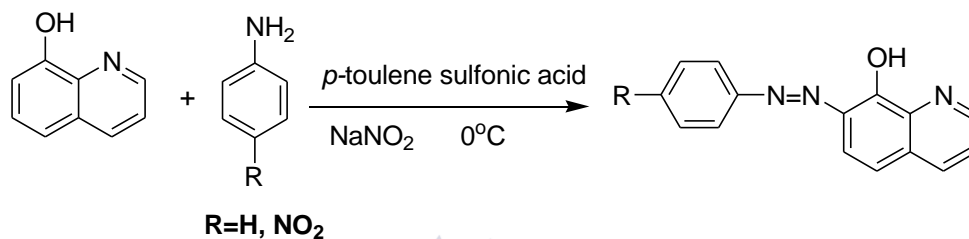
Scheme 1: Formation of aryl azo dye using para-nitroaniline or simple aniline with fluorescein.



Scheme 2: Formation of aryl azo dyes using para-nitroaniline or simple aniline with naphthalene-2,7-diol.



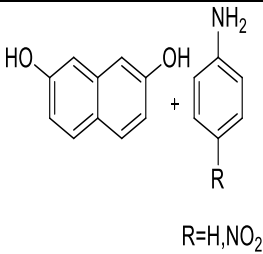
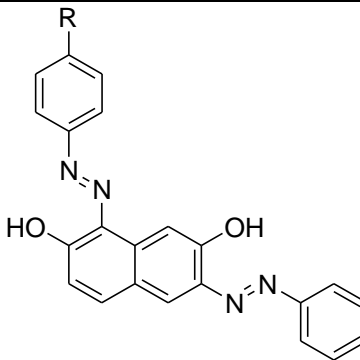
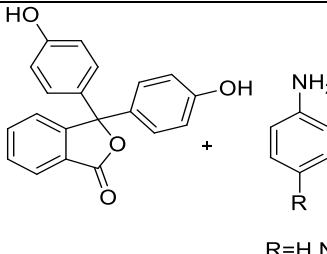
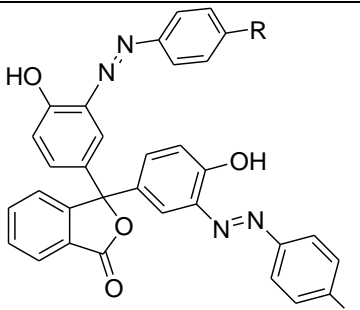
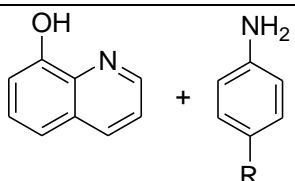
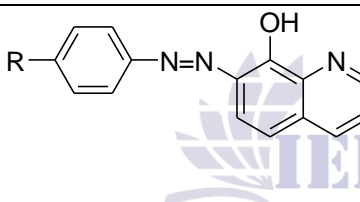
Scheme 3: Formation of aryl azo dye using para-nitroaniline or simple aniline with phenolphthalein.



Scheme 4: Formation of aryl azo dye using para-nitroaniline or simple aniline with 8-hydroxyquinoline.

Table 1: Melting points, yield, and color of the different aryl azo dyes.

Phenol derivatives and Anilines	Products	M.P	Yield	Color
<p>Reaction of phenolphthalein with an aniline derivative (R = H, NO₂).</p>	<p>Structure of the product (aryl azo dye) where the amino group of the aniline derivative has been converted to an azo group ($\text{N}=\text{N}$) and is now bonded to the phenolic ring of the phenolphthalein derivative.</p>	<p>140⁰C (When R=NO₂) 170⁰C (When R=H)</p>	<p>85%</p> <p>78%</p>	<p>Brown Red</p> <p>Dark Brown</p>

 <p>R=H, NO₂</p>		160°C (When R=NO ₂) 150°C (When R=H)	88% 76%	Brown Brown red
 <p>R=H, NO₂</p>		170°C (When R=NO ₂) 150°C (When R=H)	78% 78%	Bright Yellow Blackish Brown
 <p>R=H, NO₂</p>		157.8°C (When R=NO ₂) 154.4°C (When R=H)		

2.3 Characterization

To confirm the structure, the final products have been characterized using spectroscopic techniques such as FTIR and NMR (¹H & ¹³C). Thin-layer chromatography (TLC) was used to check the progress of the reaction and detect the product. UV light of 254 and 366 nm was used to observe TLC.

2.4 Biological Activity Evaluation

The synthesized compounds were evaluated for their antihemolytic, antibacterial, and antibiofilm properties using established protocols as detailed below:

2.4.1 Antihemolytic Assay

The antihemolytic potential was assessed based on procedures adapted from previous studies (Learnal & Prakash, 2014; Komolafe, 2017). Initially, EDTA was diluted using isotonic saline solution (0.9% NaCl) and centrifuged at 1000 rpm for 10 min. Whole

blood samples were subsequently collected in EDTA-containing tubes. Red blood cells (RBCs) were isolated via centrifugation, washed, and resuspended in phosphate-buffered saline (PBS) at pH 7.4 to prepare a uniform erythrocyte suspension. Test compounds were introduced to the suspension and incubated at ambient temperature for 5 min to induce oxidative stress and membrane damage.

Following treatment, hemolysis was monitored by measuring the absorbance at 540 nm using a spectrophotometer. Quercetin served as the reference standard, and measurements were compared against appropriate controls.

2.4.2 Antibacterial Assay

The standard disc diffusion method, outlined by Cavalieri et al. (2005), was used to determine antibacterial efficacy. The synthesized compounds were applied onto sterile filter paper discs placed on

agar plates inoculated with target bacterial strains. Zones of inhibition were then measured to provide a comparative analysis of antibacterial potency.

2.4.3 Antibiofilm Assay

In addition to the disc diffusion analysis, the microbial biofilm formation inhibition potential of the compounds was tested against *B. subtilis* and *E. coli*. Each well of a sterile microtiter plate was loaded with 100 μ L of nutrient broth, 100 μ L of the test sample, and 10 μ L of the bacterial suspension. Plates were incubated at 37 °C for 18 h. Post incubation, non-adherent cells were removed by washing twice with 220 μ L of PBS. Adherent biofilms were fixed using 99% methanol for 15 min, then stained with 7% crystal violet solution for 10 min to visualize biofilm biomass.

3. Results and Discussion

3.1 Spectral Data

Spectral data of fluorescein and para-nitroaniline containing azo-dye: (RS-1)

IR (KBr) cm^{-1} 3350, 3050, 1730, 1550, 1450.49, 1150, 1250; ^1H NMR (500 MHz, DMSO-d_6) δ (ppm) 8.21 (d, 1H); 7.99-7.92 (m, 6H); 7.79-7.79 (m, 2H); 7.71-7.66 (m, 2H); 7.59-7.57 (d, 2H); 7.15 (d, 2H); 6.69 (d, 2H); 6.58-6.57 (d, 2H); 6.55-6.53 (d, 2H); 2.27 (s, 1H); ^{13}C NMR (125 MHz, DMSO-d_6) 168.7, 155.64, 151.91, 145.2, 137.87, 135.6, 135.4 130, 128.9, 128, 126.3, 125.4, 125.3, 124.6, 112.7, 109.5, 102.2.

Spectral data of fluorescein and aniline containing Azo-dye: (RS-2)

IR (KBr) cm^{-1} 3350, 3050, 1725, 1500, 1450, 1250, 1238; ^1H NMR (500 MHz, DMSO-d_6) δ (ppm) 8.20 (d, 2H), 7.89-7 (d, 1H), 7.78-7.73 (m, 6H), 7.71-7.70 (m, 2H), 7.24-7.23 (m, 4H), 7.12-7.11(d, 4H), 6.77-6.76 (d, 4H), 2.27 (s, 3H); ^{13}C NMR (125 MHz, DMSO-d_6) 168.7, 159.4, 152.4, 151.8, 145, 138, 135.5, 130, 129, 128.9, 128.1, 126.1, 125.5, 124.5, 123.9, 121.6, 112.6, 109.5, 102.2, 83.11.

Characterization data of phenolphthalein and aniline containing Azo-dye: (RS-3)

IR (KBr) cm^{-1} 3350, 3000, 1730, 1500, 1450, 1250, 1200; ^1H NMR (500 MHz, MeOD, δ (ppm): 11.02 (s, 1H), 8.65 (d, 2H), 7.91-7.70 (m, 3H), 7.60 (d,

1H), 7.32 (m, 1H); ^{13}C NMR (125 MHz, MeOD), δ (ppm): 169.0, 157.4, 152.5, 145.2, 137.9, 134.7, 131.0, 129.5, 129.4, 129.1, 128.1, 128, 125.5, 125.2, 125.1, 124.3, 121.6, 115.1, 113.7, 91.3.

Characterization data of phenolphthalein and para-nitroaniline containing Azo-dye: (RS-4)

IR (KBr) cm^{-1} 3350, 3000, 1730, 1550, 1450, 1250, 1150; ^1H NMR (500 MHz, DMSO-d_6): δ (ppm)8.20(d,2H),7.89-7(d,1H)7.78-7.73(m,6H)7.71-7.70(m,2H),7.24-7.23(m,4H)7.12 7.11(d,4H)6.77-6.76(d,4H)2.27(s,3H), ^{13}C NMR (125 MHz, MeOD): δ (ppm) 170.7, 157, 153, 143.141, 140 , 134, 131, 129, 128.4, 128.2, 125.5, 125.4, 124.9, 124.1, 119.3, 114.7, 92.5.

3,6-dihydroxy-2,5-bis(E-(4-nitrophenyl)diazenyl)naphthalene:(RS-5)

IR (KBr) cm^{-1} 3350, 3000, 1550, 1450, 1410, 1250, 1150; ^1H NMR (500 MHz, DMSO-d_6): δ (ppm) 9.86 (s, 2H), 8.31 (s, 1H), 7.97 (d, 1H), 7.91 (d, 4H), 7.69 (d, 1H), 7.56 (t, 4H), 7.32 (t, 2H), 7.14 (d, 1H), 6.95 (s, 1H), 6.87 (d, 1H), 6.62 (d, 1H), 6.55 (d, 1H), 6.44 (s, 1H), 6.30 (d, 1H), 6.10 (d, 1H); ^{13}C NMR (125 MHz, DMSO-d_6) 156.9, 143.4, 141.8, 138.2, 129.8, 127.3, 127, 113.7.

1,6-bis (E)-phenyldiazenyl)naphthalene-2,7-diol:(RS-6)

IR (KBr) cm^{-1} 3350, 3000, 1550, 1450, 1150; ^1H NMR (500 MHz, MeOD, δ , ppm): 7.9 (d, 10H), 8.20 (d, 2H), 7.89 (d, 1H), 7.78-7.73 (m, 1H), 7.75 (d, 1H), 7.71-7.70 (m, 2H), 7.68 (d, 1H), 7.65 (d, 1H), 7.50 (d, 1H), 7.47 (m, 1H), 7.45 (m, 1H), 7.30 (s, 1H), 7.12 (d, 2H), 6.77 (d, 2H), 6.34 (s, 1H); ^{13}C NMR (125 MHz, MeOD, δ , ppm): 172.9, 159.9, 146.4, 143.5, 141.8, 141.7, 137.1, 131.8, 130.8, 129.8, 128.6, 126, 123, 121, 119, 116, 115, 107.

7-(4-Nitro phenyldiazene)-8-hydroxy quinolone: (RS-7)

IR (KBr) cm^{-1} 3330, 1439, 1617, 1559, 1345, 1222; ^1H NMR (500 MHz, DMSO-d_6 , δ (ppm): 10.5 (s, 1H), 8.5 (d, 1H), 7.8 (d, 1H), 7.5 (m, 2H), 7.4 (d, 2H), 8.5 (d, 2H); ^{13}C NMR (125 MHz, DMSO-d_6 , δ , ppm): 169, 157, 156, 152, 144, 138, 136, 135, 134, 131, 129, 128, 127, 125, 124, 115, 93, 91.

7-(phenyldiazeno)-8-hydroxy quinolone:(RS-8)

IR (KBr) cm^{-1} 3442, 3047, 1624, 1579, 1507; ^1H NMR (500 MHz, DMSO-d_6 , δ (ppm): 10.3 (s, 1H), 8.8 (d, 2H), 7.8(m, 3H), 7.5(m, 5H), 7(m, 4H); ^{13}C NMR (125 MHz, DMSO-d_6 , δ , ppm): 160, 158, 150, 148, 145, 135, 132, 130, 129, 128, 125, 124.

The structures of the synthesized azo dyes containing fluorescein and para-nitroaniline (RS-1), phenolphthalein, and para-nitroaniline (RS-4) were confirmed by IR, ^1H NMR, and ^{13}C NMR spectroscopic techniques.

RS-1 (Fluorescein-based Azo Dye)

In the IR spectrum of RS-1, the broad absorption band at 3350 cm^{-1} corresponds to $-\text{OH}$ or $-\text{NH}$ stretching vibrations. The band observed at 3050 cm^{-1} indicates aromatic C-H stretching. In contrast, the strong peak at 1730 cm^{-1} is assigned to the carbonyl (C=O) stretching vibration, confirming the presence of a carboxylic or lactone moiety in the fluorescein structure. The absorptions at 1550 cm^{-1} and 1450 cm^{-1} can be attributed to C=C stretching in the aromatic rings and possibly to the azo ($-\text{N=N}-$) group. The 1250 cm^{-1} and 1150 cm^{-1} peaks suggest C-O and C-N stretching modes, respectively.

The ^1H NMR spectrum revealed multiple aromatic signals in the range $\delta\ 6.53\text{--}8.21\text{ ppm}$. The downfield doublet at $\delta\ 8.21\text{ ppm}$ (1H) likely arises from an aromatic proton adjacent to an electron-withdrawing nitro group. Multiplets between $\delta\ 7.92\text{--}7.66\text{ ppm}$ (total of $\sim 10\text{H}$) confirm the presence of multiple aromatic rings. Signals at $\delta\ 6.69\text{--}6.53\text{ ppm}$ (multiple doublets, each integrating for 2H) are consistent with substituted aromatic systems. A singlet at $\delta\ 2.27\text{ ppm}$ (1H) could be due to a proton adjacent to a heteroatom, possibly in a hydroxyl environment, or a methyl group if present in a different tautomeric form.

The ^{13}C NMR spectrum supports this interpretation, with a signal at 168.7 ppm corresponding to the carbonyl carbon. Peaks in the $155.6\text{--}102.2\text{ ppm}$ range are assigned to aromatic and phenolic carbons, while signals around 112.7 and 109.5 ppm further confirm substituted aromatic systems. These diverse chemical shifts are consistent with an extended conjugated aromatic system, typical of azo dyes involving fluorescein- and nitro-substituted anilines.

RS-4 (Phenolphthalein-based Azo Dye)

The IR spectrum of RS-4 is similar in key features to that of Compound A, characteristic bands at 3350 cm^{-1} ($-\text{OH}/-\text{NH}$), 3000 cm^{-1} (aromatic C-H), and 1730 cm^{-1} (C=O stretch). The 1550 and 1450 cm^{-1} bands correspond to aromatic C=C and azo functionalities, respectively, while the 1250 and 1150 cm^{-1} peaks confirm C-O and C-N stretching vibrations, indicative of phenolic and amine components.

In the ^1H NMR spectrum, multiple aromatic proton signals were observed. The doublet at $\delta\ 8.20\text{ ppm}$ (2H) is consistent with deshielded protons adjacent to a nitro group. Broad multiplets between $\delta\ 7.89\text{--}7.70\text{ ppm}$ (accounting for $\sim 9\text{H}$) support the presence of a dense, aromatic framework. The signals from $\delta\ 7.24$ to 6.76 ppm (several doublets and multiplets integrating to over 10H) suggest multiple substituted benzene rings with varying electronic environments. The singlet at $\delta\ 2.27\text{ ppm}$ (3H) is likely attributed to a methyl group, possibly on a nitrogen or aromatic ring, which may result from structural modifications during diazo coupling.

The ^{13}C NMR spectrum revealed a peak at 170.7 ppm , which is characteristic of a carbonyl carbon, likely originating from the phenolphthalein core. Resonances between 157 and 92.5 ppm reflect a combination of aromatic, phenolic, and possibly quinoid-type carbons. The chemical shifts around 114.7 and 92.5 ppm indicate substituted aromatic carbons in varied environments, supporting the successful integration of the azo moiety with the phenolphthalein and para-nitroaniline fragments.

Overall, the spectroscopic data confirmed the successful synthesis of both azo dyes. The observed spectral features agree with the proposed structures and functional groups expected from the diazo coupling of para-nitroaniline with fluorescein and phenolphthalein, respectively. The differences in chemical shifts and IR band intensities reflect the variation in electronic environments owing to the distinct core structures (fluorescein vs. phenolphthalein), which may influence their dyeing behavior and photophysical properties.

3.2. Bioactivities

3.2.1 Antibacterial Activity

Figure 1 presents absorbance values indicating the antibacterial activity of various RS samples (RS-01 to RS-08) against *B. subtilis* and *E. coli*. Higher absorbance values than the respective positive controls (0.135 for *B. subtilis* and 0.114 for *E. coli*) suggest greater bacterial growth inhibition. For *B.*

subtilis, RS-05 showed the highest absorbance (0.982), indicating strong antibacterial activity, while RS-08 showed the least (0.232). Similarly, for *E. coli*, RS-07 and RS-08 had the highest absorbance values (0.898 and 0.894), suggesting notable inhibition. These results indicate that several RS samples exhibit significant antibacterial potential against both tested bacterial strains.

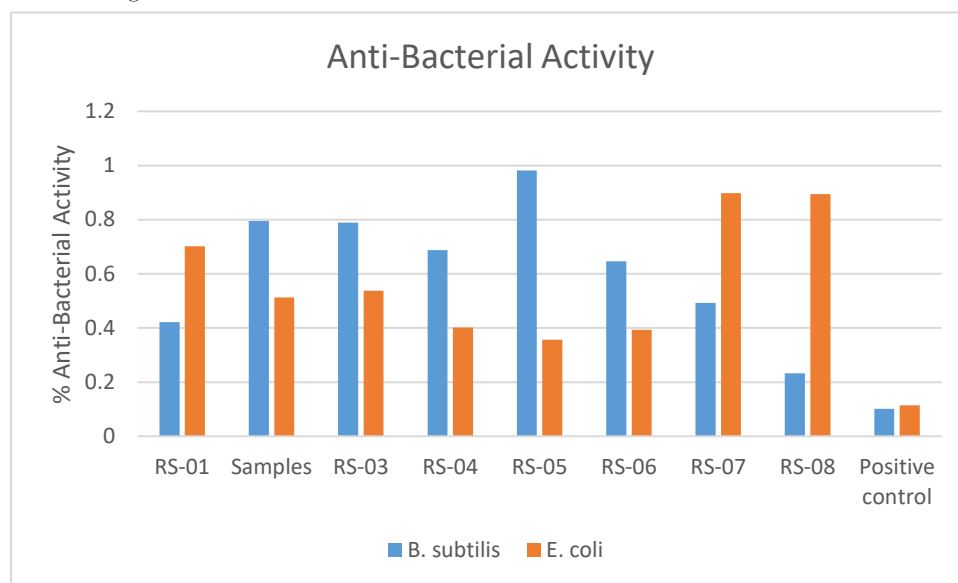


Figure 1. Antibacterial Activity of the Compounds.

3.2.2 Antibiofilm Activity

The biofilm inhibition assay results for eight test samples (RS-01 to RS-08) were evaluated against two bacterial strains: *B. subtilis* and *E. coli*. The ability of each compound to inhibit biofilm formation was measured and expressed as a percentage, with a known positive control included for comparison in Figure 2.

Against *B. subtilis*, the inhibition levels varied significantly among the tested samples. RS-08 exhibited the highest inhibitory effect, achieving 76.11% inhibition, notably close to the positive control at 89.6%. This suggests strong anti-biofilm potential. RS-01 and RS-07 also showed promising activity, with 56.54% and 49.23% inhibition, respectively. Moderate inhibition was observed with RS-06 (33.47%) and RS-04 (29.25%), while RS-02 and RS-03 displayed similar, lower levels of activity around 18%. Interestingly, RS-05 showed a slightly negative

value (-1.13%), indicating it had no effect or possibly promoted biofilm formation in *B. subtilis*.

In contrast, the activity profile against *E. coli* differed notably. The most effective sample was RS-05, showing 54.35% inhibition, followed closely by RS-06 and RS-04 with 49.74% and 48.59%, respectively. RS-02 and RS-03 also demonstrated moderate inhibition (34.4% and 31.33%), while RS-01 had minimal effect at 10.23%. Notably, RS-07 and RS-08 failed to inhibit biofilm formation and showed negative values (-14.83% and -14.32%), suggesting potential biofilm-promoting activity. The positive control for *E. coli* biofilm inhibition was 85.42%, providing a reference for high inhibitory efficacy.

These findings indicate that while specific samples showed promising anti-biofilm activity against one bacterial species, their efficacy varied against another, highlighting the strain-specific effects of these compounds.

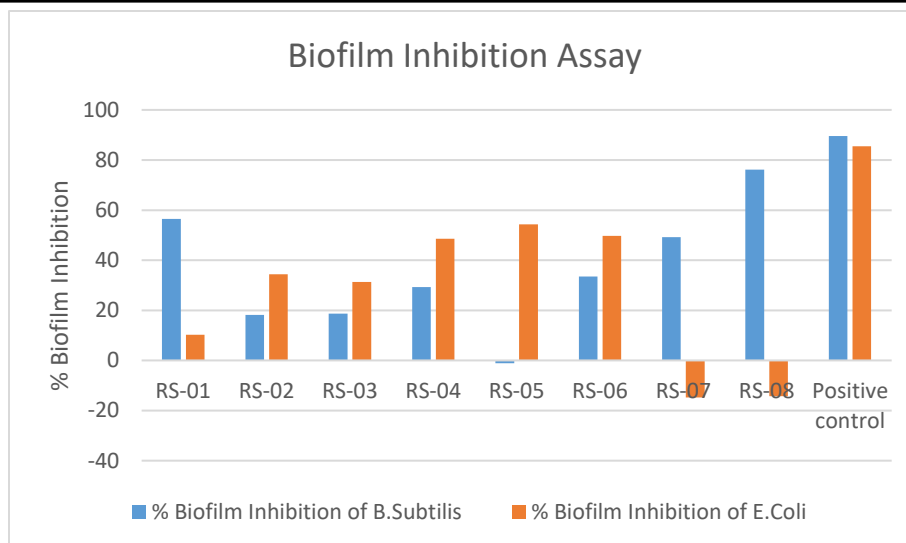


Figure 2. Biofilm inhibition activity of the synthesized compounds.

3.2.3 Anti-hemolytic activity

The anti-hemolytic activity of the synthesized compounds was assessed by evaluating the percentage of hemolysis induced in erythrocytes under oxidative stress in **Figure 3**. RS-08 exhibited the most promising anti-hemolytic effect among the tested compounds, showing the lowest hemolysis at 18.51%, indicating strong membrane-stabilizing potential. Compounds RS-02 (26.15%), RS-04 (25.30%), and RS-07 (25.13%) also demonstrated good protective activity, with hemolysis percentages

well below 30%. On the other hand, RS-01 (45.33%), RS-03 (45.84%), and RS-06 (39.39%) showed moderate hemolytic activity, suggesting a lesser but noticeable protective effect. RS-05 recorded the highest hemolysis among the test samples at 56.20%, indicating weaker anti-hemolytic potential. For comparison, the positive control (inducing complete oxidative damage) showed 88.29% hemolysis, while the negative control exhibited no hemolysis, confirming the reliability of the assay conditions.

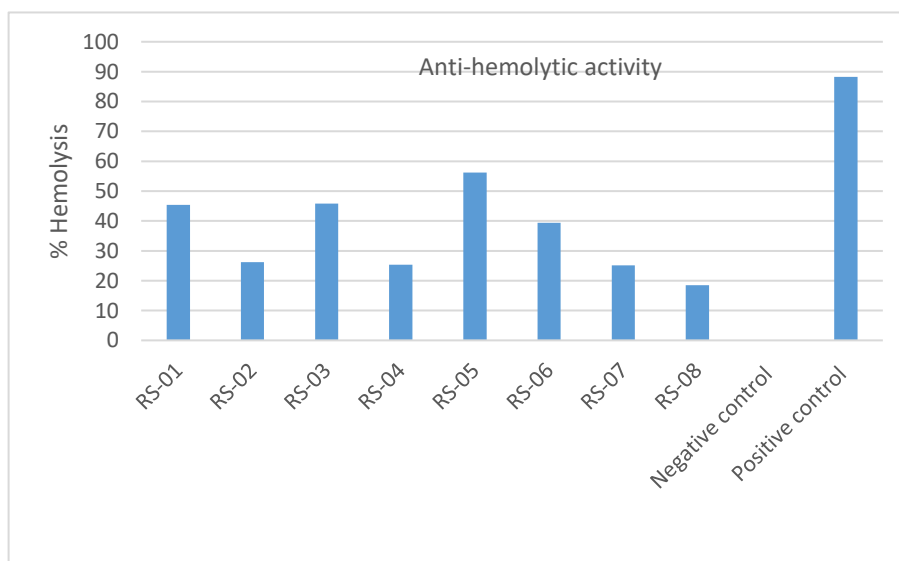


Figure 3. Anti-hemolytic activity of the compounds.

4. Conclusion

This research shows an effective solvent-free mechanochemical approach for synthesizing aryl azo dyes, eliminating reliance on harmful organic solvents and corrosive acidic reagents. The approach is rooted in the principles of green chemistry and offers many practical advantages, including ease of operation, cost efficiency, and reduced environmental footprint. These dyes were produced in excellent yields (ranging from 88% to 95%) and showed intense coloration, high thermal stability, and structural integrity. These characteristics were certified through TLC analysis and confirmed by comprehensive spectroscopic techniques such as FTIR and NMR spectroscopy.

Beyond their chemical characteristics, the synthesized compounds were subjected to biological evaluations. Many derivatives showed notable inhibition of biofilm formation by *B. subtilis* and *E. coli*, pointing to their potential antibacterial abilities. Hemolytic activity further demonstrated a range of cytotoxic effects, with compound RS-08 standing out due to its minimal hemolytic response, indicating promise for biomedical applications. This convergence of environmentally benign production and biological potential extends the utility of azo dyes beyond traditional domains, suggesting applications in antimicrobial treatment and biosensing technologies. Overall, this study emphasizes the potential of solvent-free methodologies in sustainable synthesis and the design of multifunctional materials. Future work will explore structural modifications to enhance bioactivity and expand these dyes' application in medical and environmental fields.

REFERENCES

1. Zollinger, H. (2003). Color Chemistry: Syntheses, Properties, and Applications of Organic Dyes and Pigments. Wiley-VCH.
2. Hunger, K. (2007). Industrial Dyes: Chemistry, Properties, Applications. Wiley-VCH.
3. Clarke, M. J. (2006). "Metallopharmaceuticals and the Anticancer Activity of Platinum Complexes". Coord. Chem. Rev., 236, 209-233.
4. Shore, J. (2002). Colorants and Auxiliaries: Volume 1: Colorants. Society of Dyers and Colourists.
5. Muthyala, R. (1997). Chemistry and Applications of Leuco Dyes. Springer.
6. Mudassir, M. A., et al. (2021). Hyperbranched Polyethylenimine-Tethered Multiple Emulsion-Templated Hierarchically Macroporous Poly(acrylic acid)-Al₂O₃ Nanocomposite Beads for Water Purification". ACS Appl. Mater. Interfaces. 13, 27400-27410.
7. Mudassir, M. A., et al. (2017). Development of Silver-Nanoparticle-Decorated Emulsion-Templated Hierarchically Porous Poly(1-vinylimidazole) Beads for Water Treatment". ACS Appl. Mater. Interfaces. 9, 24190-24197.
8. Gowri, M., et al. (2012). "Synthesis and Characterization of Azo Dyes for Textile Applications". J. Chem. Pharm. Res., 4(1), 1035-1039.
9. Rovina, K., et al. (2017). "Toxicity, Detection and Analysis of Azo Dyes in Food". TrAC Trends Anal. Chem., 85, 1-10.
10. Freeman, H. S., & Peters, A. T. (2000). Colorants for Non-Textile Applications. Elsevier.
11. Gómez, V., et al. (2007). "Removal of Synthetic Dyes from Wastewaters". Water Res., 41(15), 3411-3423.
12. Mudassir, M. A., et al. (2021). "Fundamentals and Design-Led Synthesis of Emulsion-Templated Porous Materials for Environmental Applications". Adv. Sci. 8, 2102540.
13. Mudassir, M. A., et al. (2023). "Emulsion-Derived Porous Carbon-Based Materials for Energy and Environmental Applications". Renew. Sustain. Energy Rev. 185, 113594.
14. Anastas, P. T., & Warner, J. C. (1998). Green Chemistry: Theory and Practice. Oxford University Press.
15. Sheldon, R. A. (2017). "Green Chemistry and Resource Efficiency: Towards a Green Economy". Green Chem., 19(1), 18-43.

16. Clark, J. H., & Macquarrie, D. J. (2002). *Handbook of Green Chemistry and Technology*. Blackwell Science.
17. Baláž, P. (2013). *Mechanochemistry in Nanoscience and Minerals Engineering*. Springer.
18. Kousar, S., et al. (2025). "Synthesis and Characterization of Thioamidoalkyl Fluorescein Analogs for Antibacterial Activity and Molecular Docking Analyses". *Curr. Organocatal.*, ISSN: 2213-3372. <http://dx.doi.org/10.2174/0122133372319377241218122708>.
19. James, S. L., et al. (2012). "Mechanochemistry: Opportunities for New and Cleaner Synthesis". *Chem. Soc. Rev.*, 41(1), 413–447.
20. Tan, D., & García, F. (2019). "Mechanochemistry: An Emerging and Sustainable Strategy in Synthesis". *Chem. Soc. Rev.*, 48(8), 2274–2292.
21. Frišić, T., et al. (2020). "Mechanochemical Reactivity and Reactors for Green Synthesis". *Nat. Rev. Chem.*, 4, 241–255.
22. Wang, G.-W. (2013). "Mechanochemical Organic Synthesis". *Chem. Soc. Rev.*, 42(18), 7668–7700.
23. Kaupp, G. (2009). "Mechanochemistry: The Varied Applications of Mechanical Bond-Breaking". *CrystEngComm*, 11(3), 388–403.
24. Varma, R. S. (2014). "Microwave-Assisted Reactions in Green Chemistry". *Pure Appl. Chem.*, 76(4), 701–707.
25. Kappe, C. O. (2004). "Controlled Microwave Heating in Modern Organic Synthesis". *Angew. Chem. Int. Ed.*, 43(46), 6250–6284.
26. Loupy, A. (2006). *Microwaves in Organic Synthesis*. Wiley-VCH.
27. Sekkat, Z., & Knoll, W. (2002). *Photoreactive Organic Thin Films*. Academic Press.
28. Natansohn, A., & Rochon, P. (2002). "Photoinduced Motions in Azo-Containing Polymers". *Chem. Rev.*, 102(11), 4139–4176.
29. Bandara, H. M. D., & Burdette, S. C. (2012). "Photoisomerization in Different Classes of Azobenzene". *Chem. Soc. Rev.*, 41(5), 1809–1825.
30. Sharma, V., et al. (2015). "Azo Dye-Based Sensors: Colorimetric and Fluorometric Applications". *Sens. Actuators B*, 211, 295–317.
31. Pang, X., et al. (2014). "Azo-Polymer Materials for Data Storage". *Adv. Mater.*, 26(41), 6349–6369.
32. Yu, Y., et al. (2003). "Smart Coatings Based on Azo Polymers". *Nature*, 425(6954), 145.
33. Ali, H., & Ahmad, W. (2019). "Biological Potential of Azo Compounds". *Curr. Med. Chem.*, 26(23), 4281–4301.
34. Mishra, A., et al. (2008). "Azo Dyes as Anticancer Agents". *J. Med. Chem.*, 51(24), 7391–7399.
35. Kumar, R., et al. (2012). "Design and Development of Azo Compounds for Biological Use". *Bioorg. Med. Chem.*, 20(5), 1580–1586.

